Spatial distribution of lamin A determines nuclear stiffness and stress-mediated deformation

Luv Kishore Srivastava[1], Zhaoping Ju[2], Ajinkya Ghagre[1], Allen J. Ehrlicher[1,2]*

1. **Department of Bioengineering, McGill University, Montreal H3A 0E9**
2. **Department of Anatomy and Cell Biology, McGill University, Montreal H3A 0C7**

Abstract: The nucleus is the largest organelle and information center of the cell; while we identify the diverse components of the cells as mechanotransduction elements, the deformation of the nucleus itself is emerging as a critical mechanosensory structure, suggesting that the nuclear stiffness itself is essential in determining correct responses to intracellular and extracellular stresses. A nuclear membrane protein lamin A, is a known critical component in nuclear stiffening; however, the quantitative relationship between lamin A expression and nuclear deformation is still unclear.

Here we measure the nuclear moduli as a function of lamin A expression and stress applied to the nuclei, demonstrating that in wild-type lamin A expressing cells the bulk modulus has a strong dependence on expression levels. We additionally examined the spatial variation across the nuclear envelope in lamin A expression and deformation, revealing that local areas of the nuclear envelope with higher expression levels of lamin A have correspondingly lower local deformations and that increased lamin A expression levels result in a narrower distribution of smaller deformations. We also find that the measured deformations are largest along the minor axis of the nucleus, demonstrating a mechanical anisotropy in nuclear compressibility.

Introduction: The nucleus is the largest organelle and the information center of the cell, integrating diverse biochemical cues for proper cell function[1]. In addition to biochemical cues, the nucleus has an increasingly clear role as a mechanosensory structure in the cell[2]. Nuclear mechanotransduction is a process by which the nucleus detects mechanical cues and converts

them to biochemical signals which alter the physiology of the cell. As a mechanosensor, the nucleus's stiffness is key to determining specific deformations in response to applied stresses. The nucleus is generally significantly stiffer than the cytoplasm, with an effective Young's modulus ranging from 1–10kPa[3,4], however, these values are not fixed, and multiple factors may cause nuclear stiffness to change significantly. For example, the stiffness of nuclei varies 5-fold during cell division[5], and in stem cells, the stiffness can increase 6-fold over the differentiation process[6]. Also, in many types of cancers, the structure and shape of the nucleus are significantly altered, with the stiffness of the nucleus vastly reduced[7]. Thus, diverse factors and conditions impact the nuclear stiffness; however, these are often the result of nuclear envelope architecture changes[8].

The nuclear envelope is composed of double-membraned bilipid layers with a 30–50nm perinuclear space between the membranes. The outer nuclear membrane is connected to the endoplasmic reticulum, whereas the inner membrane is held in place by a consortium of more than 50 membrane proteins. Some of the proteins present in the inner nuclear membrane include emerin, SUN1, SUN2, and lamin associated proteins[9]. Lamins are type V intermediate filaments localized under the nuclear membrane. The inner membrane is held in place by the underlying nuclear lamina, which is mainly composed of A type and B type lamins. Lamin A has a profound effect on the stiffness of the nucleus, but lamin B shows very little or no effect on the nuclear stiffness, thus making lamin A a dominant component in nuclear mechanics[10].

Numerous studies have illustrated the significance of lamin A in determining the stiffness of the nucleus. Substrate strain experiments showed that in lamin A knockout cells, nuclei show 50% more deformation compared to wild-type cell nuclei[11]. For the same cells, magnetic bead microrheology showed that in lamin A knockout cells, the beads are displaced 30% more

compared to wild-type cells. Previous studies have also shown that in lamin A knockout cells, nuclei are more fragile, as much more nuclei ruptured in lamin A knockout cells compared to wild type cells with an increase in intranuclear pressure. Furthermore, 3T3 Fibroblast cells transfected with wild type lamin A showed 40–50% less deformation in both intact and isolated nuclei on vertical nanopillars[12]. Nuclei isolated from cells transfected with shRNA for lamin A showed 1.5–1.7 times more bead displacement compared to wild type nuclei in magnetic bead microrheology indicating the role of lamin A in determining the stiffness of the nucleus[13]. The relationship between lamin A expression and nuclear stiffness directly affects the behavior of the cell; as an example, lamin A overexpression hinders 3D cell migration through micropores[14]; however, it seems to facilitate 2D migration as wild type cells are marginally faster than lamin A knockout cells[15]. The vast majority of these studies have looked at binary treatments of lamin A, i.e., parsing cells into groups of overexpression, wild type, or knock-down, but the quantitative scaling of nuclear stiffness, and corresponding nuclear deformation as a function of lamin A expression remains unknown.

Expression of lamin A is highly variable, and changes in different stages of cell cycle[16], increasing in stem cell differentation[17], and as a function of microenvironment stiffness[18]. In addition to expression levels, the distribution of lamin A appears heterogeneous with the formation of foci and honeycomb patterns observed in the nuclear envelope[19]. Thus, heterogenous expression level and spatial distribution of lamin A may result in anisotropic deformation of the nuclei, even under isotropic pressure.

It remains unknown how the spatial heterogeneity of lamin A affects nuclear deformation. Studies to date have focused on comparing gross changes in ensemble population lamin A expression via over-expression or suppression[20], but have not examined the quantitative

dependence of nuclear stiffness on lamin A expression, or the impact of the spatial distribution of lamin A.

To understand the quantitative impact of lamin A structure on nuclear mechanics, here we measure the deformability and bulk moduli of nuclei as a function of lamin A expression. We identify a mechanical anisotropy of bulk compression, leading to increasing relative compression in the major, minor, and z axis, respectively. At the sub-micron level, we quantify the spatial distribution of lamin A and show that locally dense lamin A structures attenuate local deformation, providing heterogeneous nuclear deformations under uniform nuclear stresses.

Methodology

Quantification of lamin A expression using antibodies and lamin A chromobody: To quantify the total lamin A present in the cell, the nucleus was stably transfected with GFP tagged lamin A chromobody (Chromtek) and to verify the chromobody as a quantitative metric, we compared its fluorescence with antibody staining (Atto-647N Sigma) as a gold standard (see supplementary information Fig. 5). For this, lamin A chromobody transfected cells were seeded onto gridded coverslips, fixed, permeabilized and stained with Atto-647 lamin A antibodies, and then imaged with a 63X/1.4 NA oil immersion objective on a confocal microscope (Leica SP8). Fluorescence colocalization was determined using Pearson's coefficient for 10 cells (see supplementary information Fig. 6).

Cell culture & modulating nuclear lamin A expression: NIH 3T3 cells were cultured following standard protocols in DMEM media supplemented with 10% FBS and 1% Penicillin-Streptomycin antibiotic. To increase the expression of lamin A in intact cells we transfected cells with m-Cherry tagged plasmid DNA for lamin A (Addgene Cat. No. 55068), whereas to knock-

down lamin A expression we transfected the cells with RFP tagged inducible shRNA construct for lamin A (Dharmacon). All cells were co-transfected with GFP tagged lamin A chromobody, which labels the total lamin A present on the nuclear membrane without affecting its expression (see supplementary information Fig. 7).

Quantification of nuclear bulk moduli: We exposed the cells attached on coverslips with 1%, 2.5%, 5% and 10% 400 Da polyethylene glycol (PEG 400, Sigma) thus, exerting 404kPa, 493kPa, 656kPa, 857kPa, and 1MPa respectively for 25 minutes to reach an equilibrium of compression[22], followed by acquiring confocal microscopy XYZ-stacks (63x 1.4NA, Leica SP8). The cells compress due to the osmotic pressure exerted by the hypertonic solution causing an efflux of water[23], and this change in volume is measured and used to determine the bulk modulus by the relation $B = -\Delta P / (\Delta V/V)$ where, B= bulk modulus, ΔP = osmotic pressure, ΔV= change in volume and V = original volume[24].

3-D volume measurement of nuclei: GFP tagged lamin A chromobody cells were imaged using a 63X/1.4 NA oil immersion objective on a Leica SP8 confocal microscope with a z-step size of 0.3µm. 3-D visualization and measurement were carried out using ImageJ software. Before 3D measurement, the nuclear images were deconvolved using the 'Iterative deconvolve 3D' plugin in ImageJ. We measured nuclear volumes by counting the number of voxels after thresholding the nuclei and when multiplied by the size of each voxel gives the volume of the thresholded region. To measure the major, minor and z-axis, we imaged XYZ stacks for different time intervals post PEG addition. Then the stacks were then summed in the Z dimension using 'z-project' plugin in image J. This was followed by fitting the z-projections into an ellipse and calculating the major and minor axis for different time intervals.

Nuclear strain mapping: To measure the local strain on the nuclear membrane, a custom-made MATLAB code[25] was modified and used. Briefly, the code utilizes a fast Fourier transform (FFT) based cross-correlation formulation in conjunction with the iterative deformation method (IDM). FIDVC calculates the displacement between the images of pre and post 2.5% PEG 400 (493kPa) exposed GFP tagged lamin A chromobody nucleus by tracking the pixel intensities of chromobody fluorescence. We mapped these local displacements with the lamin A expressions of the respective coordinates.

Results:

Lamin A stiffens the nucleus: To measure the bulk compressibility of the nuclei, we exposed cell nuclei with varying lamin A expression with 400 Da PEG. Since PEG is impermeable across the cell membrane, it creates a hyperosmotic environment for the cell and nucleus. This hyperosmotic pressure leads to cellular water efflux, resulting in cell and nuclear compression, as shown in Fig. 1(a). This compression is exclusively due to the expulsion of water as the cell and nuclei regain their original volume when returned to isotonic media[23,24]. Previous studies clearly show that under external osmotic pressure cell and nuclear compression are highly correlated. An external osmotic pressure applied to the cell induces nuclear volume changes along with the concentration of intracellular macromolecules, thus providing a hyperosmotic environment to the nucleus and exerting compressive forces on it[23,24]. Fig. 1(b) shows the pressure-volume curve for wild type 3T3 cells at different PEG 400 concentrations exerting different osmotic pressures.

This is also reflected in the bulk moduli as calculated from the change in nuclear volume, as shown in Fig. 1(c) where the cell expressing more lamin A becomes stiffer. The bulk modulus for the highest lamin A expressing cell at the highest exerted osmotic pressure is 3.48Mpa.

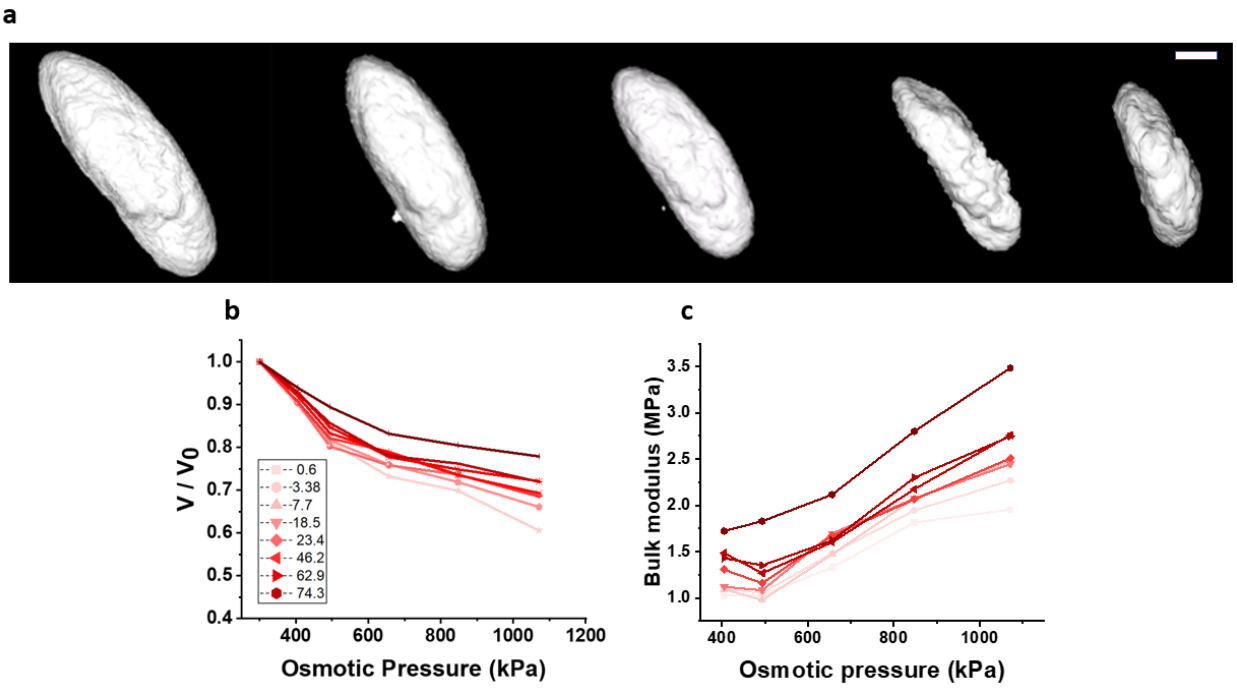

Figure 1: **Hyperosmotic compression of the nucleus in 3T3 Fibroblast cells: a,** 3D reconstruction of an example nucleus within a cell at osmotic pressures of 300kPa, 400kPa, 493kPa, 650kPa and 1MPa (left to right). **b,** Normalized nuclear volumes of 3T3 cells transfected with lamin A chromobody for wild type cells showing that stiffness increases as the protein expression increases. **c,** Bulk moduli of 3T3 cells transfected with lamin A chromobody for wild type showing that stiffness increases as the protein expression increases. (n=8) (scalebar=3µm)

Anisotropy in nuclear deformation: To measure the anisotropic nuclear deformation, we exposed the cells transfected with lamin A chromobody to PEG and imaged with confocal microscopy (Leica SP8) after 25 minutes of PEG addition. Fig. 2(a) shows an example nucleus in YZ and XZ planes before (top) and after (bottom) adding PEG. Fig. 2(b) shows the corresponding nuclear deformations in major, minor, and z-axis. These data reveal strongly anisotropic nuclear deformation where the deformation in z-axis was highest, followed by minor axis, and the least deformation in the major axis. To understand the dynamics of nuclear deformation under stress, we imaged the nuclei every 60 seconds after PEG addition. Fig. 2(c) shows major and minor axis as a function of time after the addition of PEG. Here, the nucleus

quickly flattens in the z-axis, resulting in a transient expansion along the major and minor axes, which contract after 6 minutes.

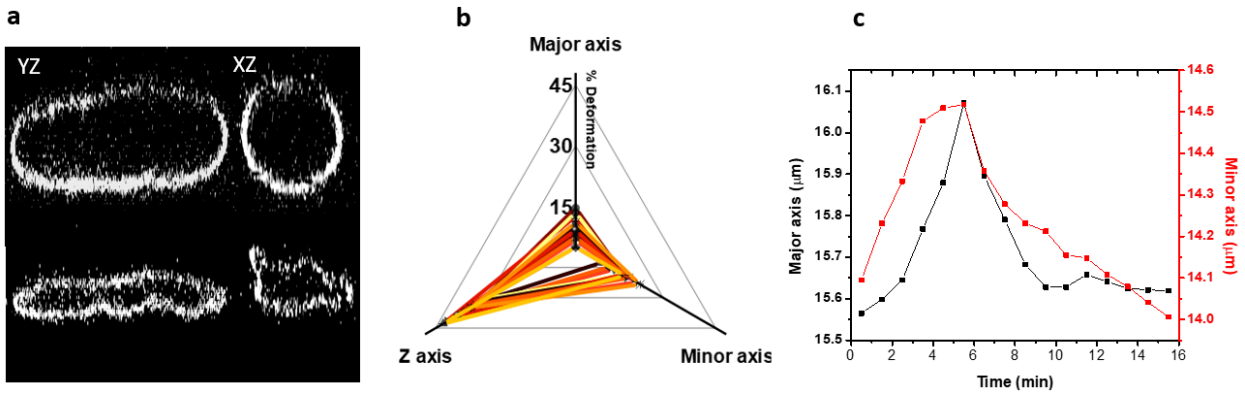

Figure 2: Anisotropy in nuclear compression under PEG: a, Example of a wild type nuclei in YZ and XZ plane before PEG addition (top) and after PEG addition (bottom) showing large deformation in the z axis. **b,** Nuclear deformation percentage along the major, minor and z axis in wild type nuclei (n=15) showing higher deformation along z axis compared to the major and minor axis. **c,** Major and minor axis in wild type cell nucleus after adding PEG showing that the wild type nucleus first stretches after PEG addition increasing the major and minor axis followed by a reduction in the major and minor axis.

Lamin A spatial heterogeneity and nuclear strain mapping: Fig. 3(a) shows that lamin A expression is heterogeneous across the nuclear membrane. This heterogeneity is quantified and shown in Fig. 3(b). The distribution of lamin A is found to be heterogeneous; in a large population of cells, lamin A expression was found to be slightly higher along the major axis than the minor axis. Fig. 3(c) shows the normalized variance across the nuclear membrane as a function of lamin A in wild type cells. To eliminate the possibility of the gain contributing to the variance with an increase in lamin A fluorescence, the fluorescence of images were increased and did not show any role of gain contributing to increase in variance (see supplementary information Fig. 8).

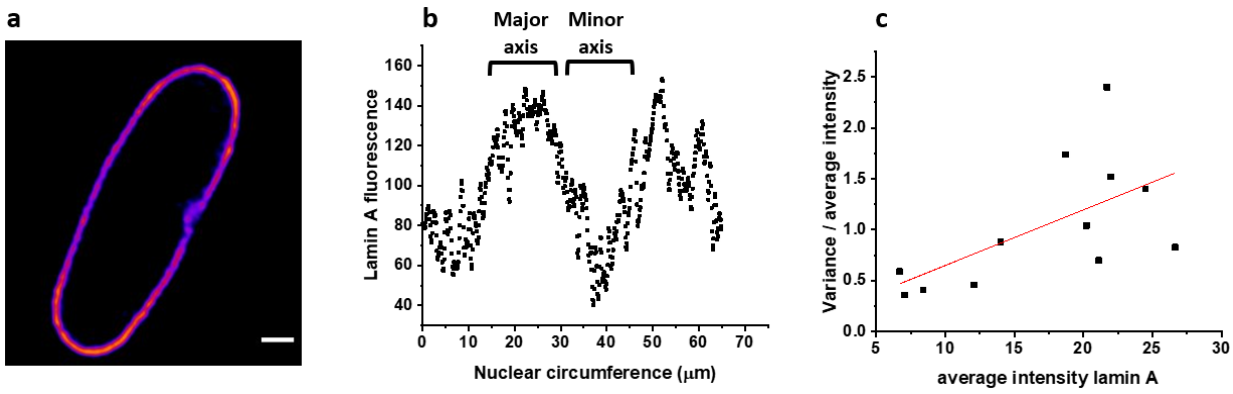

Figure 3: Spatial heterogeneity of lamin A in the nucleus increases with expression. a, Example 3T3 fibroblast cells transfected with lamin A chromobody showing variability in the spatial distribution along a cross-section nuclear membrane (scalebar = 3μm). **b,** Example characteristic scatter plot of fluorescence along the nuclear circumference. **c**, Normalized variance of lamin A chromobody fluorescence (n=12) showing that spatial heterogeneity of lamin A increases with expression levels.

Fig. 4(a) and (b) show the nuclear deformation map and lamin A distribution in the X-Y plane along the nuclear membrane, whereas Fig. 4(c) shows the nuclear deformation map (top) and lamin A distribution (bottom) in the Y-Z plane. These images demonstrate the inverse relationship between spatial variations of Lamin A and deformation; where there is low lamin A expression, the deformation appears to be maximum and vice-versa. To quantify these spatial variations, we plotted lamin A fluorescence with respective deformations along the nuclear circumference, as shown in Fig. 4(d). Fig. 4(e) shows the deformation as a function of the fraction of lamin A present at the nuclear membrane. These results show that nuclear deformation is least where lamin A expression is maximum, and maximal in regions lower in lamin A. Fig 4(f) shows the relationship between the ratio of osmotic stress applied to the deformation, measured as a function the lamin A expression yields the effective lamin A stiffness. Thus demonstrating that the stiffness increases as lamin A expression increases locally. While this finding is consistent in all cells measured, some cells also presented low deformation

in regions of low lamin A expression (see supplementary information Fig. 9), which may be attributed to the mechanical anisotropy of the underlying chromatin[26]. We observed this mechanical anisotropy of the nucleus also along the major and minor axes of the nucleus, where the minor axis is deformed to a larger extent as shown in Fig. 4(g).

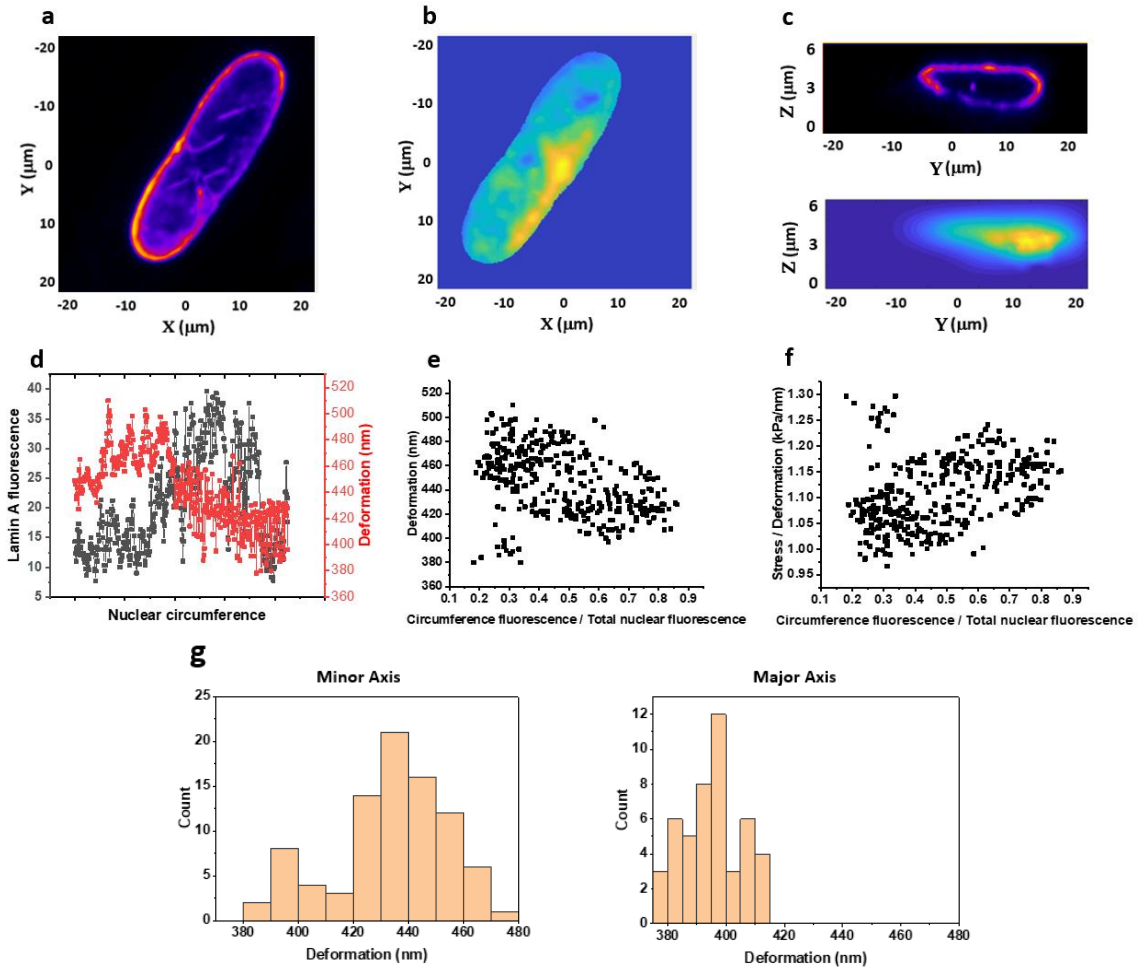

Figure 4: Local nuclear deformation as a function of lamin A distribution in 3T3 fibroblasts. a, Example strain X-Y plane map of a 3T3 nucleus under 493kPa stress (scalebar = 5µm). **b,** Lamin A distribution along the nuclear membrane in X-Y plane. **c,** Lamin A distribution (top) and Y-Z strain map (bottom) along the nuclear membrane. **d,** Lamin A fluorescence and nuclear deformation along the nuclear membrane. **e,** Deformation plotted against the ratio of lamin A fluorescence at the membrane and total nuclear fluorescence. **f,** Ratio of stress to deformation (yielding

stiffness) plotted against the ratio of lamin A fluorescence at the membrane and total nuclear fluorescence. **g,** Histogram of deformation distribution along major and minor axis.

Discussion: Here we have quantitatively examined the role of wild type lamin A in nuclear mechanics. Using osmotic pressure, we applied precisely controlled stresses and measured global volumetric changes. Decomposing these volumetric changes, we identify anisotropic deformation of the nucleus showing maximum deformation in z-axis followed by minor axis and then major axis, respectively. Inspecting the expression of lamin A more closely, we found distinct spatial variations in concentration within the nuclear envelope; interestingly, the heterogeneity of lamin A density increased with expression level in wild type. We suspected that these spatial variations in concentration would lead to similar spatial variations in nuclear stiffness. By quantifying the spatial variations of lamin A density and comparing this with a sub-micron resolution deformation map of the nucleus, we indeed found a strong inverse correlation between local lamin A concentration and deformation, demonstrating that the spatial variation of lamin leads to heterogeneous deformation. Also, the local deformations along the minor axis were found to be larger than the corresponding major axis, which was consistent with our previous observation, as seen in bulk deformation of the nuclei.

Thus, the expression of lamin A is critical in nuclear mechanics; however, variations in the form of lamin A also impact its structure and may impact nuclear mechanics. Mutations in the *lmna* gene lead to altered isoforms of lamin A resulting in a group of pathological conditions called as 'laminopathies'; one example of such a disorder is the Hutchinson Gilford Progeria Syndrome (HGPS) which affects the nuclear architecture and stiffness[27]. Since the nuclear lamina connects chromatin, an abnormal nuclear stiffness might lead to unusual nuclear deformation inducing epigenetic changes in the chromatin[28,29], thus leading to altered gene expression, which might

result in dysfunction and pathology[30]. Thus, the stiffness of the nucleus and its deformation is an essential parameter as it directly affects the gene expression.

Another factor contributing to nuclear stiffness is the tethering of chromatin with the nuclear lamina[31]. Since the chromatin can be present as heterochromatin (highly compact non-expressing chromatin conformation) and euchromatin (non-compact expressing chromatin conformation), it contributes to the mechanical anisotropy of the nuclear envelope[32]. While lamin A is the major contributor to nuclear stiffness under high mechanical stress, under small stresses, chromatin has a crucial role as well[26]. More condensed heterochromatin regions are stiffer and experience less deformation compared to euchromatin[33], making chromatin dynamics additionally important in nuclear mechanotransduction. Nevertheless, the physical association between the nuclear lamina and the chromatin, as well as the relationship between nuclear deformation and its direct effect on epigenetic changes are still unclear and could prove to be essential in relating nuclear mechanics with various pathological conditions.

Previous mechanotransduction studies have shown that mechanical forces can lead to translocation of mechanosensitive proteins such as YAP from the cytoplasm to the nucleus under nuclear tension[34], which affects properties like cell proliferation and differentiation in stem cells. Lamin A could prove to be a critical factor in elucidating this relationship as it directly affects the nuclear stiffness and its deformation. By manipulating lamin A expression, relating the change in nuclear mechanics, and measuring downstream effects, we may better understand how nuclear stiffness determines cellular fates, thus providing novel mechanics-centered strategies to correct defects in disease.

Acknowledgments: The authors thank members of Christian Frank's lab, University of Wisconsin, for assistance with MATLAB FIDVC. AJE acknowledges support from NSERC (RGPIN/05843-2014, EQPEQ/472339-2015, RTI/00348-2018), CIHR (Grant # 143327), and the Canadian Foundation for Innovation (Project #32749).

References

1. Lamond, A. I. & Earnshaw, W. C. Structure and function in the nucleus. *Science* **280**, 547–553 (1998).
2. Kirby, T. J. & Lammerding, J. Emerging views of the nucleus as a cellular mechanosensor. *Nat. Cell Biol.* **20**, 373–381 (2018).
3. Vaziri, A. & Mofrad, M. R. K. Mechanics and deformation of the nucleus in micropipette aspiration experiment. *J. Biomech.* **40**, 2053–2062 (2007).
4. Caille, N., Thoumine, O., Tardy, Y. & Meister, J. J. Contribution of the nucleus to the mechanical properties of endothelial cells. *J. Biomech.* **35**, 177–187 (2002).
5. Chu, F.-Y., Haley, S. C. & Zidovska, A. On the origin of shape fluctuations of the cell nucleus. *Proc. Natl. Acad. Sci.* **114**, 10338–10343 (2017).
6. Pajerowski, J. D., Dahl, K. N., Zhong, F. L., Sammak, P. J. & Discher, D. E. Physical plasticity of the nucleus in stem cell differentiation. *Proc. Natl. Acad. Sci. U. S. A.* **104**, 15619–15624 (2007).
7. Lin, H.-H. *et al.* Mechanical phenotype of cancer cells: cell softening and loss of stiffness sensing. *Oncotarget* **6**, (2015).
8. Bell, E. S. & Lammerding, J. Tumour Progression. **95**, 449–464 (2017).
9. Hetzer, M. W. The nuclear envelope. *Cold Spring Harb. Perspect. Biol.* **2**, a000539 (2010).
10. Dechat, T., Adam, S. A., Taimen, P., Shimi, T. & Goldman, R. D. Nuclear Lamins. 1–22 (2010).
11. Lammerding, J. *et al.* Lamin A / C deficiency causes Tema Grupo defective nuclear mechanics and mechanotransduction. *J. Clin. Invest.* **113**, 370–378 (2004).
12. Hanson, L. *et al.* Vertical nanopillars for in situ probing of nuclear mechanics in adherent cells. *Nat. Nanotechnol.* **10**, 554–562 (2015).
13. Guilluy, C. *et al.* Isolated nuclei adapt to force and reveal a mechanotransduction pathway in the nucleus. *Nat.Cell Biol.* **16**, 376–381 (2014).
14. Harada, T. *et al.* Nuclear lamin stiffness is a barrier to 3D migration, but softness can limit survival. *J. Cell Biol.* **204**, 669–682 (2014).
15. Wang, Y., Jiang, J., He, L., Gong, G. & Wu, X. Effect of lamin-A expression on migration and nuclear stability of ovarian cancer cells. *Gynecol. Oncol.* **152**, 166–176 (2019).
16. Moir, R. D. *et al.* Review: The dynamics of the nuclear lamins during the cell cycle - Relationship between structure and function. *J. Struct. Biol.* **129**, 324–334 (2000).
17. Schirmer, E. C. & Gerace, L. The stability of the nuclear lamina polymer changes with the composition of lamin subtypes according to their individual binding strengths. *J. Biol. Chem.* **279**, 42811–42817 (2004).
18. Crisp, M. *et al.* Coupling of the nucleus and cytoplasm. *J. Cell Biol.* **172**, 41–53 (2006).

19. Barateau, A. *et al.* A novel lamin a mutant responsible for congenital muscular dystrophy causes distinct abnormalities of the cell nucleus. *PLoS One* **12**, 1–18 (2017).

20. Lammerding, J. *et al.* Lamins a and C but not lamin B1 regulate nuclear mechanics. *J. Biol. Chem.* **281**, 25768–25780 (2006).

21. Guilak, F., Tedrow, J. R. & Burgkart, R. Viscoelastic properties of the cell nucleus. *Biochem. Biophys. Res. Commun.* **269**, 781–786 (2000).

22. Zhou, E. H. *et al.* Universal behavior of the osmotically compressed cell and its analogy to the colloidal glass transition. *Proc. Natl. Acad. Sci.* **106**, 10632–10637 (2009).

23. Guo, M. *et al.* Cell volume change through water efflux impacts cell stiffness and stem cell fate. *Proc. Natl. Acad. Sci.* (2017). doi:10.1073/pnas.1705179114

24. Adele Khavari, A. J. E. Nuclei deformation reveals pressure distributions in 3D cell clusters. *PLoS One* (2019).

25. Bar-Kochba, E., Toyjanova, J., Andrews, E., Kim, K. S. & Franck, C. A Fast Iterative Digital Volume Correlation Algorithm for Large Deformations. *Exp. Mech.* **55**, 261–274 (2015).

26. Stephens, A. D., Banigan, E. J., Adam, S. A., Goldman, R. D. & Marko, J. F. Chromatin and lamin A determine two different mechanical response regimes of the cell nucleus. *Mol. Biol. Cell* **28**, 1984–1996 (2017).

27. Goldman, R. D. *et al.* Accumulation of mutant lamin A progressive changes in nuclear architecture in Hutchinson-Gilford progeria syndrome. *Proc. Natl. Acad. Sci. U. S. A.* **101**, 8963–8968 (2004).

28. Sinha, B. *et al. Dynamic Organization of Chromatin Assembly and Transcription Factories in Living Cells*. *Methods in Cell Biology* **98**, (Elsevier Masson SAS, 2010).

29. Wang, Y., Nagarajan, M., Uhler, C. & Shivashankar, G. V. Orientation and repositioning of chromosomes correlate with cell geometry–dependent gene expression. *Mol. Biol. Cell* **28**, 1997–2009 (2017).

30. Koehler, F. *et al.* Epigenetic deregulation of lamina-associated domains in Hutchinson-Gilford Progeria Syndrome. *bioRxiv* 520403 (2019). doi:10.1101/520403

31. Schreiner, S. M., Koo, P. K., Zhao, Y., Mochrie, S. G. J. & King, M. C. The tethering of chromatin to the nuclear envelope supports nuclear mechanics. *Nat. Commun.* **6**, 1–13 (2015).

32. Berendes, H. D. & Keyl, H. G. Distribution of DNA in heterochromatin and euchromatin of polytene nuclei of Drosophila hydei. *Genetics* **57**, 1–13 (1967).

33. Hampoelz, B. & Lecuit, T. Nuclear mechanics in differentiation and development. *Curr. Opin. Cell Biol.* **23**, 668–675 (2011).

34. Driscoll, T. P., Cosgrove, B. D., Heo, S. J., Shurden, Z. E. & Mauck, R. L. Cytoskeletal to Nuclear Strain Transfer Regulates YAP Signaling in Mesenchymal Stem Cells. *Biophys. J.* (2015). doi:10.1016/j.bpj.2015.05.010